Revealing the electronic structure of a carbon nanotube carrying a supercurrent

Jean-Damien Pillet, Charis Quay, Pascal Morfin, Cristina Bena, A. Levy Yeyati, Philippe Joyez

Revealing the electronic structure of a carbon nanotube carrying a supercurrent

J.-D. Pillet[a], C. H. L. Quay[a], P. Morfin[b], C. Bena[c,d], A. Levy Yeyati[e] and P. Joyez[a]

[a]*Quantronics Group,*

Service de Physique de l'Etat Condensé,

CNRS URA 2426, IRAMIS, CEA

F-91191 Gif-sur-Yvette, France

[b]*Laboratoire Pierre Aigrain (LPA), CNRS UMR 8551,*

Université Pierre et Marie Curie (Paris VI) - Université Denis Diderot (Paris VII) - Ecole Normale Supérieure de Paris (ENS Paris)

[c]*Laboratoire de Physique des Solides, CNRS UMR 8502,*

Université Paris-Sud, Bât. 510, F-91405 Orsay, France

[d]*Institut de Physique Théorique, CEA/Saclay,*

CNRS URA 2306, Orme des Merisiers,

F-91191 Gif-sur-Yvette, France and

[e]*Departamento de Física Téorica de la Materia Condensada C-V,*

Universidad Autónoma de Madrid, E-28049 Madrid, Spain.

Carbon nanotubes (CNTs) are not intrinsically superconducting but they can carry a supercurrent when connected to superconducting electrodes [1–4]. This supercurrent is mainly transmitted by discrete entangled electron-hole states confined to the nanotube, called Andreev Bound States (ABS). These states are a key concept in mesoscopic superconductivity as they provide a universal description of Josephson-like effects in quantum-coherent nanostructures (e.g. molecules, nanowires, magnetic or normal metallic layers) connected to superconducting leads [5]. We report here the first tunneling spectroscopy of individually resolved ABS, in a nanotube-superconductor device. Analyzing the evolution of the ABS spectrum with a gate voltage, we show that the ABS arise from the discrete electronic levels of the molecule and that they reveal detailed information about the energies of these levels, their relative spin orientation and the coupling to the leads. Such measurements hence constitute a powerful new spectroscopic technique capable of elucidating the electronic structure of CNT-based devices, including those with well-coupled leads. This is relevant for conventional applications (e.g. superconducting or normal transistors, SQUIDs [3]) and quantum information processing (e.g. entangled electron pairs generation [6, 7], ABS-based qubits [8]). Finally, our device is a new type of dc-measurable SQUID.

First envisioned four decades ago [9], ABS are electronic analogues of the resonant states in a Fabry-Pérot resonator. The cavity is here a nanostructure and its interfaces with superconducting leads play the role of the mirrors. Furthermore, these "mirrors" behave similarly to optical phase-conjugate mirrors: because of the superconducting pairing, electrons in the nanostructure with energies below the superconducting gap are reflected as their time-reversed particle – a process known as Andreev Reflection (AR). As a result, the resonant standing waves – the ABS – are entangled pair of time-reversed electronic states which have opposite spins (Fig. 1a); they form a set of discrete levels within the superconducting gap (Fig. 1b) and have fermionic character. Changing the superconducting phase difference φ between the leads is analoguous to moving the mirrors and changes the energies $E_n(\varphi)$ of the ABS. In response, a populated ABS carries a supercurrent $\frac{2e}{h}\frac{\partial E_n(\varphi)}{\partial \varphi}$ through the device, while states in the continuous spectrum (outside the superconducting gap) have negligible or minor contributions in most common cases [5]. Therefore, the finite set of ABS generically determines Josephson-like effects in such systems. As such, ABS play a central role in mesoscopic superconductivity and can be seen as the superconducting counterpart of the Landauer channels for the normal state: in both cases, only a handful of them suffices to account for all the transport properties of complex many-electron systems such as atomic contacts or CNTs. In effect, the ABS concept quantitatively explains the Josephson effect in atomic contacts [10]; it also explains tunneling spectroscopy of vortex cores and surface states in some superconductors [11]. However, there has been to date no detailed direct spectroscopic observation of individual ABS. Interest in such spectroscopy has increased with recent proposals for using ABS as quantum bits [8], and AR as a source of entangled spin states [6].

Nanotubes are particularly good candidates for the observation of ABS. First, CNT-superconductor hybrid systems are expected to show a small number of ABS, and the typical meV energy scales involved in nanotube devices are comparable with conventional superconducting gaps. These are favourable conditions for a well-resolved spectroscopy experiment. Second, given the length of CNTs, it is possible to introduce an additional tunnel probe which enables straightforward tunneling spectroscopy [12]. Furthermore, CNTs are of fundamental interest as nearly ideal, tunable one-dimensional systems in which a wealth of phenomena (e.g. Luttinger-liquid behavior [13], Kondo effects [3, 14] and spin-orbit coupling [15]) has been observed, whose rich interplay with superconducting coupling has attracted a lot of interest [16–22].

Our sample is described in Figure 1. A CNT is well connected to two superconducting metallic contacts 0.7 µm apart, leaving enough space to place a weakly-coupled tunnel electrode in between. The electrodes are made of aluminum with a few nm of titanium as a sticking layer (see SI for details); they become superconducting below $\sim 1\,\mathrm{K}$. The two outer contacts are reconnected, forming a loop. A magnetic flux Φ threaded through the loop produces a superconducting phase difference $\varphi = \frac{2e}{h}\Phi$ across the tube. By measuring the differential conductance of the tunnel contact at low temperature ($T \sim 40\,\mathrm{mK}$) we observe (see Fig. 2a, 3a) well-defined resonances inside the superconducting gap. The energies of these resonances strongly depend on the voltage applied on the back-gate of the device, and vary periodically with the phase difference accross the CNT, a signature of ABS. From the raw measurement of the differential conductance between the tunnel probe and the loop we can extract the density of states (DOS) in the tube (see e.g. fig. 2b) through a

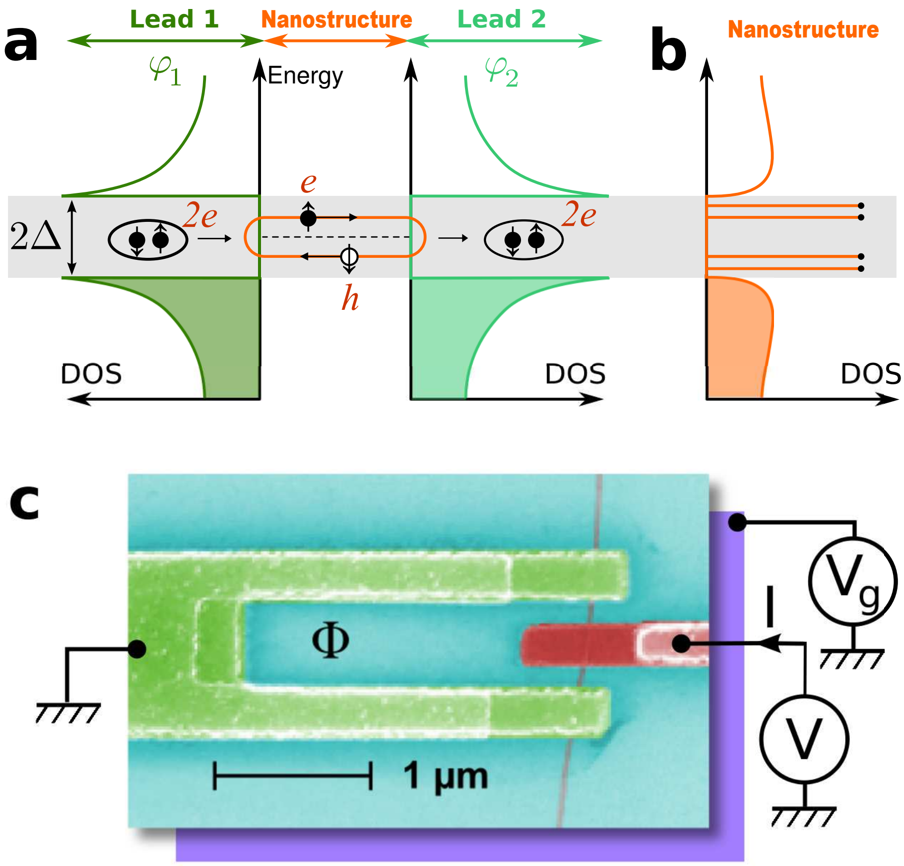

Figure 1: **a** : Generic schematic for an Andreev Bound State (ABS) in a nanostructure between two superconducting leads, which have Densities of States (DOS) with a gap Δ, and with respective superconducting phases $\varphi_{1,2}$. At energies within the superconducting gap (grey band) the Andreev reflection process (which reflects an electron (e) as a hole (h) – its time-reversed particle – and vice versa) leads to the formation of discrete resonant states of entangled $e-h$ pairs confined between the superconductors. These states –the ABS– are electronic analogues to the resonances in an optical Fabry-Pérot cavity. **b** : The local DOS in the nanostructure is thus expected to display a set of resonances in the gap at the energies of the ABS. The energies of the ABS should depend periodically on the superconducting phase difference $\varphi = \varphi_1 - \varphi_2$ which is analogous to the optical cavity length. **c** : Color-enhanced scanning electron micrograph of a device fabricated for the spectroscopy of ABS in a CNT which appears here as the thin vertical grey line. The substrate consists of highly doped silicon serving as a back gate (figured here in violet), with a 1μm-thick surface oxide layer. A grounded superconducting fork (green) is well connected to the tube, forming a loop. The measurement of the differential conductance $\partial I/\partial V$ of a superconducting tunnel probe (red) weakly connected to the tube gives acces to the density of states in the CNT, where ABS are confined. The energies of the ABS can be tuned by varying the gate voltage V_g and the magnetic flux Φ threading the loop.

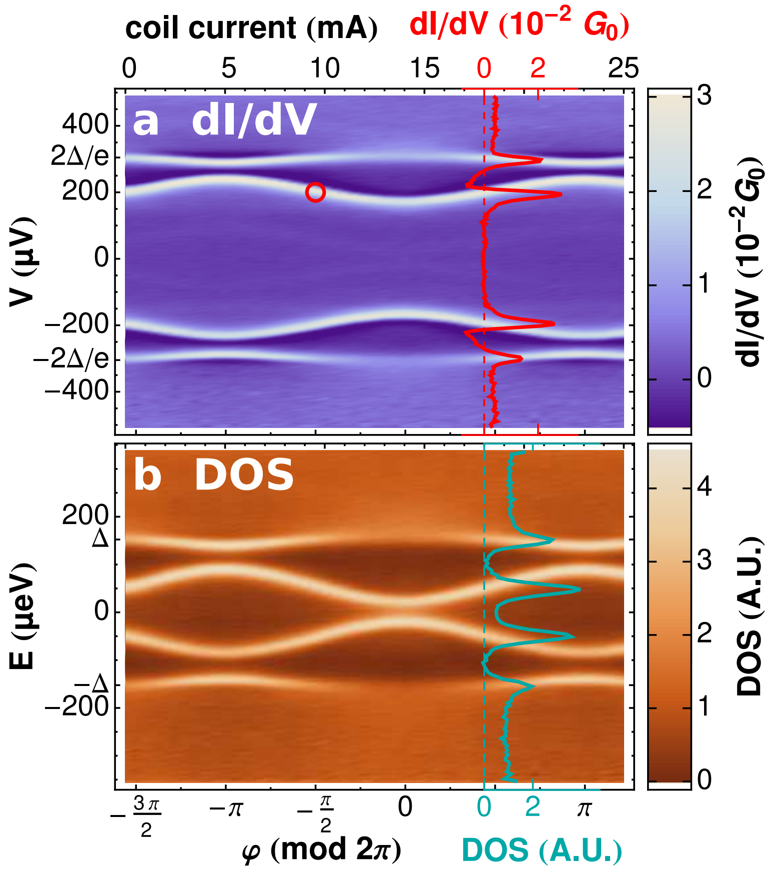

Figure 2: **a**: Differential conductance of the tunnel probe at a fixed gate voltage$V_g = -0.5\,\mathrm{V}$ as a function of the bias voltage V of the probe junction (vertical axis) and of the current in a coil (top axis) which controls the flux Φ through the loop. The sharp resonances are the signature of the ABS, and the periodicity of the pattern demonstrates that ABS coherently connect the two end contacts and are sensitive to their superconducting phase difference φ (bottom axis). The solid color traces correspond to cross sections of the data at the flux indicated by the dashed line. $G_0 = 2e^2/h$ denotes the conductance quantum. **b** DOS in the CNT as deconvolved from the data in panel a, assuming BCS DOS in the tunnel probe. The device can be operated as a dc-current SQUID magnetometer by biasing it at a point which maximize $\partial I/\partial\Phi$, as indicated by a red circle. The fact that the phase is not zero at zero current in the coil is due to a residual magnetic field in our setup.

straightforward deconvolution procedure (see SI). Figure 2 shows the dependence of the ABS spectrum on the flux in the loop at a fixed gate voltage. By dc-biasing this device at a point which maximizes $\partial I/\partial\Phi$ (see Fig. 2a), it can be used as a SQUID magnetometer which combines the advantages of Refs [23] and [3]. Being nanotube-based, our SQUID should be

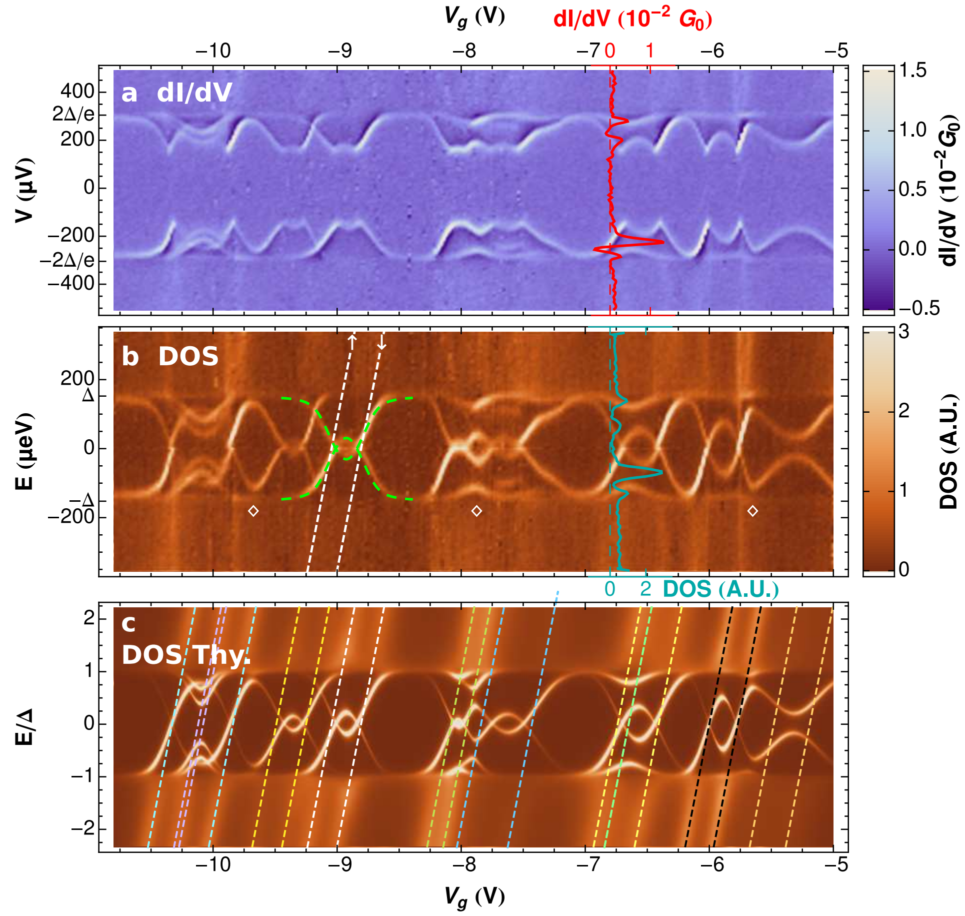

Figure 3: **Note: These color plots display well on computer screens. However, the printed appearance might be too dark depending on the printer used.**

a Gate dependence of the differential conductance of the tunnel probe. **b** DOS in the CNT as deconvolved from the data in panel a, after correcting for the gating effect of the probe junction which appears as a slight horizontal shear in panel a. The ABS form an intricate pattern of intertwined lines. Predicted from a basic quantum-dot model for the CNT, the green dotted bell-shaped lines are the positions of ABS arising from a single Spin-Split Pair of Levels (SSPL - white dashed lines) crossing the gap as the gate voltage is increased. The spin labelling indicates only the relative orientations of the spins in these levels. Most of the resonances observed in this panel have similar shapes and can be attributed to different SSPL. However, some resonances corresponding to two different SSPL are connected together where indicated by the diamonds. **c** Calculated DOS involving several coupled SSPL in a double quantum dot model. Here a SSPL is represented by a pair of dashed lines of the same color. The positions of the levels and their coupling to the electrodes were adjusted to provide best overall agreement with 2b. This simple model captures many of the observed features and shows how ABS spectroscopy allows the identification of the dot levels, and in particular of their relative spin, without applying any magnetic field.

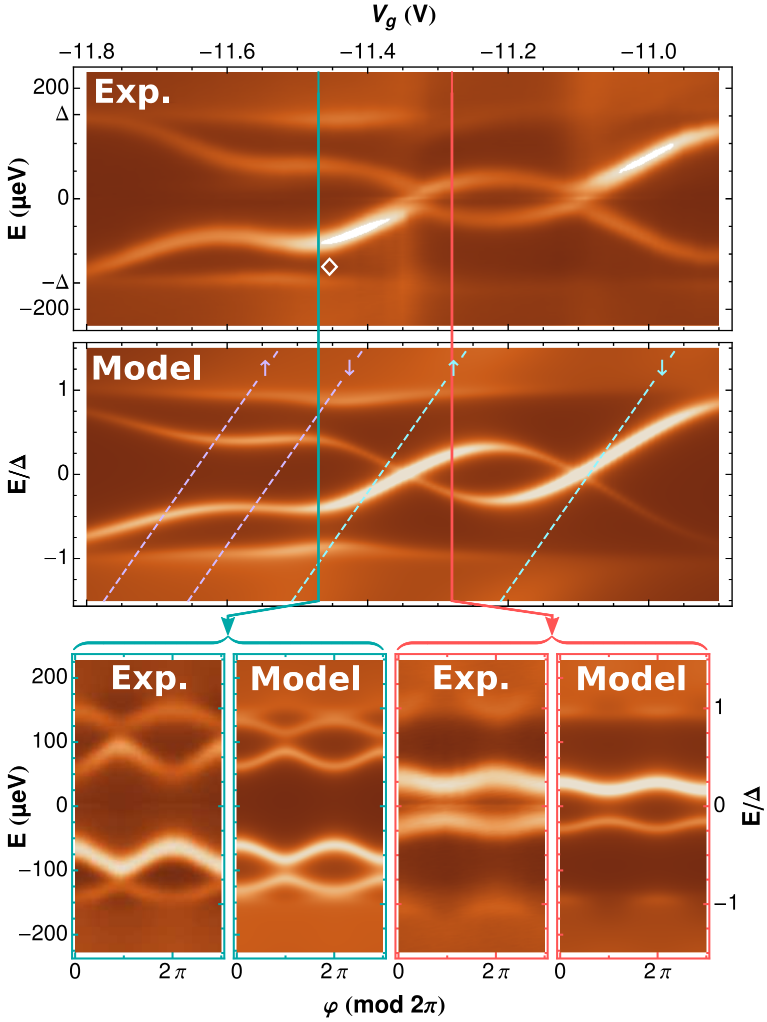

Figure 4: top panels: experimental deconvolved DOS as a function of V_g and predictions of our double quantum dot model, at phase $\varphi = 0$. Bottom pannels: experimental phase dependence taken at gate voltages indicated by the plain coloured lines in the top panels, and corresponding predictions of the model. All theoretical panels use the same set of parameters; the corresponding level positions are indicated by the dashed lines in the second pannel. The spin labelling indicates only the relative orientations of the spins in these coupled levels.

able to detect the reversal of magnetic moments of only a few Bohr magnetons[3]. At the same time, the present device can be read out with a dc current measurement (similar to [23]) and requires a single gate voltage, making it easier to operate than Ref. [3]. The gate voltage dependence of the DOS shows a pattern of resonance lines (Fig. 3b) which is more or less intricate depending on the strength of the coupling to the leads (see SI).

We now show that the ABS observed in this device arise from the discrete molecular levels in the CNT. For this we describe phenomenologically our nanotube as a Quantum Dot (QD) coupled to superconducting leads (See the SI for a detailed discussion of the model). The essential physics of ABS in this system is already captured when one considers a single orbital of the QD filled with either one or two electrons. Due to the Pauli exclusion principle, these two electrons have opposite spins and can thus be coupled by Andreev Reflection. Also, the doubly occupied state is higher in energy by an effective charging energy $\tilde{U}$ which can be determined from the experimental data. Hence, the minimal effective model consists of a Spin-Split Pair of Levels (SSPL) whose parameters are the splitting $\tilde{U}$, the mean position $\overline{E}$ of the SSPL relative to the Fermi level (which is controlled by the gate voltage V_g), and the coupling to the leads (see Fig. S1a in SI). Previous theoretical work [24, 25] has shown that there can be up to four ABS, symmetric (in position, but not in intensity) about the Fermi Level. For sufficiently large $\tilde{U}$ (respectively, $\overline{E}$), however, the two outer (respectively, all) ABS merge with the continuum and are no longer visible in the spectrum [24–26].

We now discuss the dependence of the ABS energies on the gate voltage V_g. The ABS appear as facing pairs of bell-shaped resonances centred at $\overline{E}(V_g) = 0$ and with their bases resting against opposite edges of the superconducting gap (see green dashed curves in Fig. 3b.). For large enough $\tilde{U}$ the inner resonances cross at the Fermi energy, forming a loop (Fig. 3b.). Such loops are a distinct signature of SSPL in this model (spin-degenerate levels ($\tilde{U} = 0$) cannot give loops). Most of the features observed in Fig. 3b can be identified as such pairs of bell-shaped resonances corresponding thus to different SSPL in the nanotube.

Closer inspection reveals however that adjacent resonances are sometimes coupled, forming avoided crossings (as indicated by $\diamondsuit$ symbols in Fig. 3b, 4), so that we need to consider the case where two SSPL contribute simultaneously to the spectral properties within the superconducting gap. For this, we extend the model to two serially-connected QD each containing a SSPL, with a significant hopping term in between. This model is fairly natural, given that the centre tunnel probe electrode is likely to act as an efficient scatterer. The full description of the model, the derivation of the retarded Green function from which we obtain the spectral properties, and the parameters used to produce the theoretical panels in Figures 3&4 are detailed in the SI. Assuming for simplicity that all states in the two dots are identically capacitively coupled to the gate and that the couplings to the leads are independent of V_g, we can locally reproduce most features of the gate-voltage dependence of the DOS, and simultaneously the flux dependence at fixed V_g (see fig. 4). By summing contributions of independent SSPLs and pairs of coupled SSPLs, (i.e. isolated orbitals and coupled pairs of QD orbitals) we can also reproduce the observed dependence on an extended V_g range (See Fig. 3 b & c, and discussion in the SI).

Note that a single superconducting terminal is sufficient to induce ABS in a QD (in which case, of course, there can be no supercurrent) (see Refs. [27, 28]). Given this, and in light of our analysis, we think that some features observed in Refs [29, 30] which were tentatively explained as out-of-equilibrium second order AR can now be reinterpreted as equilibrium ABS spectroscopy on a QD well connected to one superconducting lead, as in Refs. [27, 28], with the second lead acting as a superconducting tunnel probe.

The agreement between experiment and theory in Figs. 3 and 4 shows that ABS spectra constitute an entirely new spectroscopic tool for QDs and CNTs. This spectroscopy provides extremely detailed information, in particular about the relative spin state of the nanotube levels without requiring high magnetic fields. Note that, in contrast to the usual Coulomb blockade spectroscopy of QDs, the energy resolution is here essentially independent of the temperature (as long as $k_B T \ll \Delta$) and of the strength of the coupling to the leads. It should therefore allow the exploration of the transition between the Fabry-Pérot (where the Luttinger-Liquid physics is expected to play a role [18, 19]) and the Coulomb blockade regimes in CNT. We also expect this new technique to be able to provide key insights in cases where simple charge transport measurements are not sufficient to fully probe the physics at work. In particular, it should allow detailed investigation of the competition between superconductivity and the Kondo effect [16] which arise for stronger couplings to the leads. Also, used in combination with an in-plane magnetic field, it could also probe spin-orbit interactions [20–22]. Finally it should be emphasized that even while our phenomenological model successfully describes the observed experimental data further theoretical work is needed in order to establish a truly microscopic theory which should predict the level splittings from the bare many-body Hamiltonian.

The information extracted from such spectroscopy may also help to optimize Field Effect Transistors, SQUIDs or even Nano Electromechanical devices based on nanotubes, by better understanding how current is carried through the device. It could also be used for evaluating recently proposed devices for quantum information processing such as entangled electron pair generation by crossed Andreev reflection [6] or ABS-based quantum bits [8]. Regarding the latter, our observation of tunable ABS is heartening even though the measured spectroscopic linewidth ($30-40\,\mu$eV FWHM) seems to question the feasability of such qubits (if it were intrinsic to the sample, it would correspond to sub-ns coherence time). The present linewidth is however likely to be caused simply by spurious noise in the experimental setup. More investigations are needed in order to assess the potential of nanotube ABS as qubits.

To summarize, we have performed the first tunneling spectroscopy of individually resolved ABS which provide a universal description for the Josephson effect in weak links. The analysis of the ABS spectrum constitutes a powerful and promising spectroscopic technique capable of elucidating the electronic structure of CNT-based devices, including those with well-coupled leads.

Acknowledgments

This work was partially supported by ANR project SEMAFAET, C'Nano projet SPLONA, Spanish MICINN under contracts NAN2007-29366 and FIS2008-04209.

The authors gratefully acknowledge discussions with the Quantronics group, Ophir Auslander, Juan Carlos Cuevas, Reinhold Egger, Milena Grifoni, Takis Kontos, Hélène le Sueur, Alvaro Martín-Rodero, Pascal Simon and Christoph Strunk.

References

[1] Kasumov, A. Y. *et al.* Supercurrents through Single-Walled carbon nanotubes. *Science* **284**, 1508–1511 (1999).

[2] Jarillo-Herrero, P., van Dam, J. A. & Kouwenhoven, L. P. Quantum supercurrent transistors in carbon nanotubes. *Nature* **439**, 953–956 (2006).

[3] Cleuziou, J. P., Wernsdorfer, W., Bouchiat, V., Ondarcuhu, T. & Monthioux, M. Carbon nanotube superconducting quantum interference device. *Nature Nanotechnology* **1**, 53–59 (2006).

[4] Pallecchi, E., Gaass, M., Ryndyk, D. A. & Strunk, C. Carbon nanotube Josephson junctions with Nb contacts. *Applied Physics Letters* **93**, 072501–3 (2008).

[5] Beenakker, C. W. J. Three "universal" mesoscopic Josephson effects. *cond-mat/0406127* (2004). Transport Phenomena in Mesoscopic Systems, edited by H. Fukuyama and T. Ando (Springer, Berlin, 1992).

[6] Recher, P., Sukhorukov, E. V. & Loss, D. Andreev tunneling, Coulomb blockade, and resonant transport of nonlocal spin-entangled electrons. *Physical Review B* **63**, 165314 (2001).

[7] Herrmann, L. G. *et al.* Carbon nanotubes as Cooper-Pair beam splitters. *Physical Review Letters* **104**, 026801 (2010).

[8] Zazunov, A., Shumeiko, V., Bratus', E., Lantz, J. & Wendin, G. Andreev level qubit. *Physical Review Letters* **90** (2003).

[9] Kulik, I. Macroscopic quantization and proximity effect in S-N-S junctions. *Soviet Physics JETP-USSR* **30**, 944–& (1970).

[10] Della Rocca, M. L. *et al.* Measurement of the Current-Phase relation of superconducting atomic contacts. *Physical Review Letters* **99**, 127005 (2007).

[11] Fischer, Ø., Kugler, M., Maggio-Aprile, I., Berthod, C. & Renner, C. Scanning tunneling spectroscopy of high-temperature superconductors. *Reviews of Modern Physics* **79**, 353 (2007).

[12] Chen, Y., Dirks, T., Al-Zoubi, G., Birge, N. O. & Mason, N. Nonequilibrium tunneling spectroscopy in carbon nanotubes. *Physical Review Letters* **102**, 036804 (2009).

[13] Bockrath, M. *et al.* Luttinger-liquid behaviour in carbon nanotubes. *Nature* **397**, 598–601 (1999).

[14] Buitelaar, M. R., Nussbaumer, T. & Schönenberger, C. Quantum dot in the Kondo regime coupled to superconductors. *Physical Review Letters* **89**, 256801 (2002).

[15] Kuemmeth, F., Ilani, S., Ralph, D. C. & McEuen, P. L. Coupling of spin and orbital motion of electrons in carbon nanotubes. *Nature* **452**, 448–452 (2008).

[16] Glazman, L. I. & Matveev, K. A. Resonant Josephson current through Kondo impurities in a tunnel barrier. *JETP Letters* **49**, 659–662 (1989).

[17] Spivak, B. I. & Kivelson, S. A. Negative local superfluid densities: The difference between dirty superconductors and dirty Bose liquids. *Physical Review B* **43**, 3740 (1991).

[18] Fazio, R., Hekking, F. W. J. & Odintsov, A. A. Josephson current through a Luttinger liquid. *Physical Review Letters* **74**, 1843 (1995).

[19] Caux, J., Saleur, H. & Siano, F. Josephson current in Luttinger Liquid-Superconductor junctions. *Physical Review Letters* **88**, 106402 (2002).

[20] Dell'Anna, L., Zazunov, A., Egger, R. & Martin, T. Josephson current through a quantum dot with spin-orbit coupling. *Physical Review B* **75**, 085305 (2007).

[21] Dolcini, F. & Dell'Anna, L. Multiple Andreev reflections in a quantum dot coupled to superconducting leads: Effect of spin-orbit coupling. *Physical Review B* **78**, 024518 (2008).

[22] Zazunov, A., Egger, R., Jonckheere, T. & Martin, T. Anomalous Josephson current through a Spin-Orbit coupled quantum dot. *Physical Review Letters* **103**, 147004 (2009).

[23] Giazotto, F., Peltonen, J. T., Meschke, M. & Pekola, J. P. Superconducting quantum interference proximity transistor. *Nature Physics* **6**, 254–259 (2010).

[24] Yoshioka, T. & Ohashi, Y. Numerical renormalization group studies on single impurity Anderson model in superconductivity: A unified treatment of magnetic, nonmagnetic impurities, and resonance scattering. *Journal of the Physical Society of Japan* **69**, 1812–1823 (2000).

[25] Vecino, E., Martín-Rodero, A. & Levy Yeyati, A. Josephson current through a correlated quantum level: Andreev states and pi junction behavior. *Physical Review B* **68**, 035105 (2003).

[26] Meng, T., Florens, S. & Simon, P. Self-consistent description of Andreev bound states in Josephson quantum dot devices. *Physical Review B (Condensed Matter and Materials Physics)* **79**, 224521–10 (2009).

[27] Deacon, R. S. *et al.* Tunneling spectroscopy of Andreev energy levels in a quantum dot coupled to a superconductor. *Physical Review Letters* **104**, 076805 (2010).

[28] Dirks, T. *et al.* Andreev bound state spectroscopy in a graphene quantum dot. *arXiv:1005.2749* (2010). URL `http://arxiv.org/abs/1005.2749`.

[29] Eichler, A. *et al.* Even-Odd effect in Andreev transport through a carbon nanotube quantum dot. *Physical Review Letters* **99**, 126602–4 (2007).

[30] Grove-Rasmussen, K. *et al.* Superconductivity-enhanced bias spectroscopy in carbon nanotube quantum dots. *Physical Review B (Condensed Matter and Materials Physics)* **79**, 134518–5 (2009).